Mixed Energy Model for a Differential Guide Mobile Robot Evaluated with Straight and Curvature Paths

Mauricio F. Jaramillo Morales and Juan B. Gómez Mendoza
Department of Electrical, Electronic and Computer Engineering, National University, Manizales, Colombia

Keywords: Energy Model, Dynamic Model, Gaussian Path Planning, Mobile Robot.

Abstract: Energy consumption is an important issue for mobile robots that carry a limited energy sources, like batteries, for a long period of time. An energy model can relate the kinematic movements of the robot with energy values, giving an estimation of the energy needed for the robot to fulfill a specific task. In this study an energy model is proposed, based on the dynamic parameters of the mobile robot, as well as the motors, given an energy value close to real energy consumption. Mixed energy model is tested with a well-known motor energy model, using the velocities related to straight and curvature paths as input. In the results, a higher energy consumption value is identified by the mixed energy model, especially when the acceleration of the mobile robot increases. Energy models are configured with P3-DX robot mobile parameters.

1 INTRODUCTION

For mobile robots, it is critical to know the amount of energy that it must carry in order to accomplish a long-term task. Many researches in the literature underline that major energy consumption is generated for the DC motor, which governs wheel movements. However, the influence that the dynamic parameters of the mobile robot can exert in total energy consumption, has been ignored (P. Tokekar and Isler, 2014), especially for the differential guide mobile robot configuration (Kim and Kim, 2008). In this paper, a goo estimation of power and energy consumption, using a mixed energy model that takes into account the DC motor and the mobile robot dynamic parameters, incorporating in a path planning, is presented. An energy model can be calculated using the mechanical and kinetic energy formulation, based on the mass and velocity of the mobile robot (Liu and Sun, 2014; G. Kladis and Guerra, 2011), or friction estimation (Dogru and Marques, 2016; Dogru and Marques, 2018). However, the energy consumption is not related to the dynamic parameters of the robot as moments of inertia. Instead, Chuy and Bensekane's investigation presents a power consumption modeling, using a 2-dimensional, second order differential equation, that describes a four wheel steering robot forces (O. Chuy Jr. and Ordonez, 2009; I. Bensekrane and Merzouk, 2017). But, the dynamic parameters of the DC motor model are no taken into account in the energy values, related for example, with motor characteristics such as voltage and torque constants.

In Kim and Tokekar's work, velocity profiles that minimize mobile robot energy consumption for a given path, is calculated (Kim and Kim, 2008; P. Tokekar and Isler, 2014). The researchers use the energy motor model as a cost function to optimize, but in the energy saving values presented, the contribution of mobile robot dynamic parameters, such as the weight of the mobile robot or load weight, is not reflected.

In this paper, the dynamic mobile robot model based on the Lagrange formalism, and the dynamic motor model based on electrical and torque characteristics, are calculated. Then, the models torque variables are mixed. Finally a space state realization (Yun and Yamamoto, 1993) is proposed, in order to expand the state variables and simplify the Lagrange multipliers. This transformation permits description of the mixed energy model with ordinary differential equations, so that energy consumption values can be calculated. In the results section, the mixed energy model is compared to the well-known energy motor model. Both models are tested, using the typical trapezoidal velocity profile for the straight path, an adapted Gaussian function for the curvature path, and a different load weights.

The rest of this paper is organized as follows: in Section 2 the mobile robot dynamic model, motor dynamic model, and mixed energy model formulation is presented. Section III presents the calculation of

Morales, M. and Mendoza, J.
Mixed Energy Model for a Differential Guide Mobile Robot Evaluated with Straight and Curvature Paths.
DOI: 10.5220/0006912004730479
In *Proceedings of the 15th International Conference on Informatics in Control, Automation and Robotics (ICINCO 2018) - Volume 2*, pages 473-479
ISBN: 978-989-758-321-6

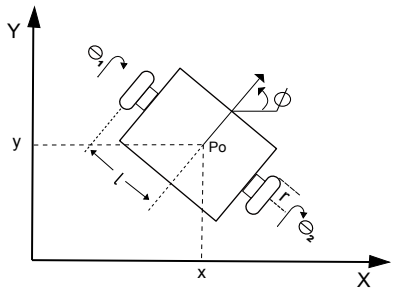

Figure 1: Schematic of the differential guide mobile robot.

the velocities, based on the desired straight and curvature paths. In Section IV, the simulations of the motor energy model and the mixed energy model are presented. Finally, conclusions are presented in Section V.

2 MIXED DYNAMIC AND ENERGY MODELS

In this section, the mixed dynamic and energy models are presented. The dynamic mobile robot model and the dynamic DC motor model are calculated . Then, both dynamic models are mixed, matching the torque values. Finally a space state realization (Yun and Yamamoto, 1993) is applied to obtain the energy model formulation.

2.1 Dynamic Mobile Robot Model based on the Lagrange Formulation

The system of nonlinear differential equations that represents the dynamic mobile robot model (Yun and Yamamoto, 1993; Yamamoto and Yun, 1994), can be determined by the Lagrange formulation to establish equations of motion for the mobile robot:

$$\frac{d}{dt}\left(\frac{\partial T}{\partial \dot{q}_i}\right) - \left(\frac{\partial T}{\partial q_i}\right) = \tau_i - a_{1i}\lambda_1 - a_{2i}\lambda_2 \quad (1)$$

with i= 1, ...4

Where:

T is the equation for mobile kinematic energy.
q is the vector of the state variables.
λ is the vector of the Lagrange's multipliers.
τ is the vector of the torques applied to the wheels.
a_{ij} are the matrix movement restriction components.

In Figure 1, the differential wheeled mobile robot is shown. The mobile robot configuration has two movement restrictions:

- The mobile robot can not move in lateral direction.

$$\dot{x}\sin\phi - \dot{y}\cos\phi = 0 \quad (2)$$

- The two driving wheels of the mobile robot, roll and do not slip.

$$\dot{x}\cos\phi + \dot{y}\sin\phi + l\dot{\phi} = r\dot{\theta}_1 \quad (3)$$

$$\dot{x}\cos\phi + \dot{y}\sin\phi - l\dot{\phi} = r\dot{\theta}_2 \quad (4)$$

Where (x,y) are the coordinates of point Po in the fixed reference coordinated frame $X-Y$, ϕ is the heading angle of the mobile robot measured from the X-axis, and θ_1, θ_2 are the angular positions of the left and right driving wheels.
The equations 3 and 4 are added and the equation 5 is obtained.

$$\dot{x}\cos\phi + \dot{y}\sin\phi = \frac{r}{2}(\dot{\theta}_1 + \dot{\theta}_2) \quad (5)$$

The equations 2 and 5 can be written in the matrix form:

$$\begin{bmatrix} a_{11} & a_{12} & a_{13} & a_{14} \\ a_{21} & a_{22} & a_{23} & a_{24} \end{bmatrix} \begin{bmatrix} \dot{x} \\ \dot{y} \\ \dot{\theta}_1 \\ \dot{\theta}_2 \end{bmatrix} = 0 \quad (6)$$

Where the components of the restriction movement matrix are:

$$\begin{bmatrix} a_{11} & a_{12} & a_{13} & a_{14} \\ a_{21} & a_{22} & a_{23} & a_{24} \end{bmatrix} = \begin{bmatrix} -\sin\phi & \cos\phi & 0 & 0 \\ -\cos\phi & -\sin\phi & \frac{r}{2} & \frac{r}{2} \end{bmatrix} \quad (7)$$

Matrix equation 6, can be expressed as:

$$A(q)\dot{q} = 0 \quad (8)$$

Where

$$q = \begin{bmatrix} q_1 \\ q_2 \\ q_3 \\ q_4 \end{bmatrix} = \begin{bmatrix} x \\ y \\ \theta_1 \\ \theta_2 \end{bmatrix} \quad (9)$$

Now, the total kinetic energy equation may be calculated with the equation:

$$\begin{aligned} T = {} & \frac{1}{2}m(\dot{x}^2 + \dot{y}^2) + m_c c d(\dot{\theta}_1 - \dot{\theta}_2)(\dot{y}\cos\phi - \dot{x}\sin\phi) \\ & + \frac{1}{2}I_w(\dot{\theta_1}^2 + \dot{\theta_2}^2) + \frac{1}{2}I_c^2(\dot{\theta}_1 - \dot{\theta}_2)^2 \end{aligned} \quad (10)$$

Equation 10 can be rewritten as:

$$T = T_t + T_r + T_m + T_w \quad (11)$$

Where:

T_t = is the kinetic energy of translation.
T_r = is the kinetic energy of rotation.
T_m = is the mobile inertia moment without wheels.
T_w = is the Wheel inertia moment.

The notation of the equation is:

b = is the displacement from each of the driving wheels to the axis of symmetry.
d = is the displacement from point P_o to the mass center of the mobile robot, which is assumed to be on the axis of symmetry.
r = is the radius of the driving wheels.
c = is a constant equal to $\frac{r}{2b}$.
m_c = is the mass of the mobile robot without the driving wheels and the rotors of the motors.
m_w = is the mass of each driving wheel plus the rotor of its motor.
I_c = is the moment of inertia of the mobile robot without the driving wheels and the rotors of the motors about a vertical axis through the intersection of the axis of symmetry with the driving wheel axis.
I_w = is the moment of inertia of each driving wheel and the motor rotor about the wheel axis.
I_m = is the moment of inertia of each driving wheel and the motor rotor about a wheel diameter.

Then, the derivatives of the Lagrange movement equation are made for i, from one to four. Finally, the nonlinear differential system equation, which represents the dynamic mobile robot model is:

$$\begin{aligned}
\lambda_1 \sin\phi + \lambda_2 \cos\phi &= m\ddot{x} - m_c d(\ddot{\phi}\sin\phi + \dot{\phi}^2\cos\phi) \\
-\lambda_1 \cos\phi + \lambda_2 \sin\phi &= m\ddot{y} + m_c d(\ddot{\phi}\cos\phi - \dot{\phi}^2\sin\phi) \\
\tau_1 - cb\lambda_2 &= m_c cd(\ddot{y}\cos\phi - \ddot{x}\sin\phi) \\
&\quad + (I_c^2 + I_w)\ddot{\theta_1} - I_c^2\ddot{\theta_2} \\
\tau_2 - cb\lambda_2 &= -m_c cd(\ddot{y}\cos\phi - \ddot{x}\sin\phi) \\
&\quad - I_c^2\ddot{\theta_1} + (I_c^2 + I_w)\ddot{\theta_2}
\end{aligned} \tag{12}$$

2.2 The Dynamic Motor Model and Dynamic Model Mixture

The dynamic model of a DC motor can be expressed by the differential equations (Electro-Craft, 1977)

$$\begin{cases} L\dfrac{d_i}{d_t} + Ri + K_w\dot{\theta} = V \\ K_t i - I_s\ddot{\theta} - \nu\dot{\theta} = \tau \end{cases} \tag{13}$$

where:
V and i = armature voltage and current.
R and L = armature resistance and inductance.
ν = is the viscous friction coefficient.
τ = is the dynamic load applied to the motor.
K_t = is the motor torque constant.
K_w = is the motor voltage constant.
I_s = is the motor shaft inertia.
$\theta = [\theta_1\ \theta_2]$ = are the angular positions of the wheels.

The first expression in 13 is voltage equation for a DC motor, and the second expression reflects torque forces applied to the DC motor. In several studies as in kim's research (Kim and Kim, 2008), the torque variable is neglected, which seems to be problematic for a real object. In the proposed model, the torque value of a DC dynamic motor model is calculated using mobile robot dynamic model.

A reduced order model can be achieved for dynamic behavior, as the electric time constant L/R may be neglected, if compared to the mechanical time constant i/ν. Hence, one may consider $L = 0$, and the first equation yields.

$$i = \frac{V - K_w\dot{\theta}}{R} \tag{14}$$

The equation (14) can be replaced in the second DC motor model equation, and by isolating τ

$$\tau = \frac{K_t}{R}V - I_s\ddot{\theta} - \left(\frac{K_t K_w}{R} + \nu\right)\dot{\theta} \tag{15}$$

In order to achieve the mixture of dynamic models, the equation for the DC motor torque τ (15), may be replaced in the dynamic robot mobile model system equation (12). Also the equation $\dot{\phi} = c(\dot{\theta_1} - \dot{\theta_2})$, calculated from the subtraction of the equations 3 and 4, may be used for ordering and writing the resulting mixed dynamic model in the following matrix equation:

$$M(q)\ddot{q} + F\dot{q} + C(q,\dot{q}) = TV - A(q)\lambda \tag{16}$$

Where:

$$M(q) = \begin{bmatrix} m & 0 & -\alpha_1 & \alpha_1 \\ o & m & \alpha_2 & -\alpha_2 \\ -\alpha_1 & \alpha_2 & I_c^2 + I_w + I_s & -I_c^2 \\ \alpha_1 & -\alpha_2 & -I_c^2 & I_c^2 + I_w + I_s \end{bmatrix}$$

$$\alpha_1 = m_c cd\sin\phi$$
$$\alpha_2 = m_c cd\cos\phi$$

$$F = \begin{bmatrix} 0 & 0 & 0 & 0 \\ 0 & 0 & 0 & 0 \\ 0 & 0 & \dfrac{K_t K_w}{R} + \nu & \\ 0 & 0 & 0 & \dfrac{K_t K_w}{R} + \nu \end{bmatrix}$$

$$C(q,\dot{q}) = \begin{bmatrix} -m_c d\dot{\phi}^2\cos\phi \\ -m_c d\dot{\phi}^2\sin\phi \\ 0 \\ 0 \end{bmatrix} \qquad T = \begin{bmatrix} 0 & 0 \\ 0 & 0 \\ \dfrac{K_t}{R} & 0 \\ 0 & \dfrac{K_t}{R} \end{bmatrix}$$

$$A(q) = \begin{bmatrix} -\sin\phi & -\cos\phi \\ cos\phi & -sin\phi \\ 0 & cb \\ 0 & cb \end{bmatrix} \tag{17}$$

2.3 The Mixed Energy Model

In this section, a space state realization is proposed (Yun and Yamamoto, 1993), in order to transform the nonlinear differential equation system that represents the mixed dynamic model, into an ordinary differential equation system, and can be tested numerically. In the process, the state space variable is increased, and the Lagrange multipliers are simplified, using the null space $S(q)$ of the restriction matrix A(q). If η is the vector of the new variables, it can be said that $A(q)S(q)\eta = 0$, and using the equation $A(q)\dot{q} = 0$ (8), it may also be said that $\dot{q} = S(q)\eta$.

The vector η was chosen as:

$$\eta = \dot{\theta} \;\; where, \;\; \dot{\theta} = [\dot{\theta_1} \quad \dot{\theta_2}]. \tag{18}$$

Being $S(q)$

$$\big[S(q)\big] = \big[s_1(q) \quad s_2(q)\big] = \begin{bmatrix} cb\cos(\phi) & cb\cos(\phi) \\ cb\sin(\phi) & cb\sin(\phi) \\ 1 & 0 \\ 0 & 1 \end{bmatrix}$$

Now, multiplying both sides of equation (16) by $S^T(q)$ and using the result $S^T(q)A(q) = 0$, it can be said that:

$$S^T(q)M(q)\ddot{q} + S^T(q)F\dot{q} + S^T(q)C(q,\dot{q}) = S^T(q)TV - S^T(q)A(q)\lambda \tag{19}$$

Derived from equation $\dot{q} = S(q)\eta$ again, term $\ddot{q}$ is obtained.

$$\ddot{q} = S(q)\dot{\eta} + \dot{S(q)}\eta \tag{20}$$

Replacing $\dot{q}$ and $\ddot{q}$.

$$S^T M(S\dot{\eta} + \dot{S}\eta) + S^T F(S\eta) + S^T C = S^T TV \tag{21}$$

Isolating $\dot{\eta}$ from (21), the following is obtained.

$$\begin{aligned} S^T MS\dot{\eta} &= S^T TV - S^T C - S^T FS\eta - S^T M\dot{S}\eta \\ \dot{\eta} &= (S^T MS)^{-1}(S^T TV - S^T C - S^T FS\eta - S^T M\dot{S}\eta) \end{aligned} \tag{22}$$

Therefore the dynamic model can be represented with these new states variables.

$$x = \begin{bmatrix} x \\ y \\ \theta_1 \\ \theta_2 \\ \dot{\theta_1} \\ \dot{\theta_2} \end{bmatrix} = \begin{bmatrix} q \\ \eta \end{bmatrix} = \begin{bmatrix} x_1 \\ x_2 \\ x_3 \\ x_4 \\ x_5 \\ x_6 \end{bmatrix} \tag{23}$$

The motion equation (22) and the equation $\dot{q} = S(q)\eta$ may be represented in the state space form

$$\dot{x} = f(x) + g(x)V \tag{24}$$

Where:

$$f(x) = \begin{bmatrix} S(q)\eta \\ -(S^T MS)^{-1}(S^T C + S^T FS\eta + S^T M\dot{S}\eta) \end{bmatrix}$$

$$g(x) = \begin{bmatrix} 0 \\ (S^T MS)^{-1}S^T T \end{bmatrix} \tag{25}$$

The voltage variable can be obtained, isolating V from equation (21).

$$V = (S^T T)^{-1}(S^T MS\dot{\eta} + S^T M\dot{S}\eta + S^T FS\eta + S^T C) \tag{26}$$

Finally, the mixed energy model can be calculated with the power integral, using the current equation (14) and the voltage equation (26).

$$E(t) = \int V(t)\; i(t)\; dt \tag{27}$$

3 VELOCITY INPUTS FOR THE ENERGY MODELS

In this section, the calculation of the angular velocities of the mobile robot wheels, related with straight and curvature paths, are shown. For the straight path, a typical trapezoidal velocity profile is used, so the robot mobile moves a specific linear distance, taking it into account that the maximum linear velocity of the robot P3-DX is 1.21 m/s, and the maximum velocities of the wheels (figure 3 (a)).

For the curvature path, a path planning from previous work, based on the Gaussian function, is proposed. In this case a cube is selected as an obstacle in the environment where the mobile robot has to travel. The base of the cube can be easily delimited by a circumference. When the mobile robot moves from an initial point to a goal point and has to avoid the obstacle, a Gaussian function is adapted to pass through the circumference, as shown in the Figure 2. The equation that represents the Gaussian function is:

$$y_d = a\exp\frac{-(x_d - f)^2}{2h^2} \tag{28}$$

Where x_d and y_d represents the desired path, f is the position of the center of the peak, and a is the height of the curve's peak. In order to accomplish the adaptation of the Gaussian function with the circumference that delimited the obstacle, f is the same center of the circumference, and a is the same radius of the circumference. The variable h is the standard deviation that controls the width of the bell. The correct estimation of this variable prevent the desired path from passing through the circumference's area.

Once the curvature path is obtained, the angular velocities of the wheels can be calculated using the

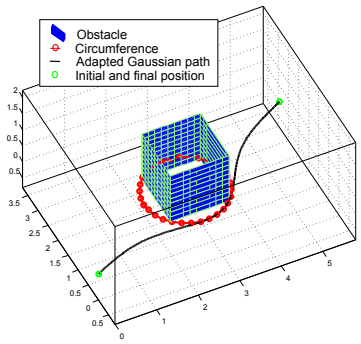

Figure 2: Adapted Gaussian path.

Table 1: Mobile parameters of the WMR, P3-DX.

Parameter	Value	Parameter	Value
r [m]	0.095	m_c [kg]	6.04
b [m]	0.165	m_w [kg]	1.48
d [m]	0		

Table 2: Motor parameters of the WMR, P3-DX.

Parameter	Value	Parameter	Value
R [ω]	0.7	K_w [(rad/s)/V]	0.88
v [Nm/(rad/s)]	0.035	K_t [Nm/A]	0.88
I_s [kgm^2]	0.0713		

kinematic inverse of the mobile robot, which is represented by the following matrix:

$$\begin{bmatrix} \dot{\theta}_1 \\ \dot{\theta}_2 \end{bmatrix} = \begin{bmatrix} \frac{\cos\phi}{r} & \frac{\sin\phi}{r} & \frac{2l}{r} \\ \frac{\cos\phi}{r} & \frac{\sin\phi}{r} & -\frac{2l}{r} \end{bmatrix} \begin{bmatrix} \dot{x}_d \\ \dot{y}_d \\ \dot{\phi} \end{bmatrix} \quad (29)$$

4 SIMULATION AND FINAL RESULTS

The energy consumption of the mixed energy model represented by Equation (27) and the motor energy model (Kim and Kim, 2008; P. Tokekar and Isler, 2014) is compared, when the mobile robot travels on straight and curvature paths, a path planning usually has these two kinds of paths. In order to set up both energy models, the mobile robot and motor parameters of the P3-DX mobile platform present in Kim's work, were used. These parameters are shown in tables 1, 2.

In the mixed energy model, when traveling a straight path, the angular velocity in both wheels has to be the same, in this case $\dot{\theta}_1 = \dot{\theta}_2 = v/r$, with v as the linear velocity of the mobile robot.

Figure 3 shows the energy consumption of both energy models , in the critical case when the mobile robot travels on a straight path of 10 meters, at the maximum trapezoidal velocity profile (1.21 m/s), with the maximum load weight (7.6 kg) allowed by the P3-DX mobile robot, and a fixed mobile weight of 6.04 kg.

Table 3: Simulation results of the energy models with a different kind of maximum linear velocities of the mobile robot.

Trapezoidal velocity	Energy value	
Maximum velocity	Motor	Mixed
0.66 m/s	53.65 J	54.51 J
0.88 m/s	71.89 J	73.68 J
1.21 m/s	98.85 J	102.9 J

Figure 3 also shows that the energy consumption values given by the mixed energy model increase faster during the acceleration of the mobile robot linear velocity, but are the same when the velocity remains at the maximum value. During deceleration, during the time corresponding to the negative phase of power consumption, a certain amount of energy is regenerated and stored in the batteries. The energy regenerated is equal to 1.05 joules for the motor energy model, and 9.07 joules for the mixed energy model.

The recovered energy allows for reduction of the total energy consumption difference between energy models. Total energy consumption in the motor energy model is 98.84 joules, and in the mixed energy model 104.3 joules. It is important to underline that the highest difference of energy consumption happens during acceleration. In this phase, energy consumption in the motor energy model is equal to 22.03 joules, and in the mixed energy model, 36.74 joules.

Table 3 shows the energy consumption values given by the energy models when the mobile robot travels on a straight path of 10 meters, with a mobile robot weight of 6.04 kg, with a fixed load weight of 3.76 kg and with different maximum set of velocities of the trapezoidal velocity profile of the mobile robot.

As the energy models depends of the kinematic mobile robot model, energy consumption raises in both models, when the maximum velocity profile increases as well. However, the energy values are higher in the mixed energy model because only this model depends on the dynamic parameters of the robot as moments of inertia and weight.

It is for this reason that in Table 4, only the mixed energy model is considerably affected in its energy consumption value, when the trapezoidal velocity is fixed at a velocity of 0.88 m/s, and the load weight increases.

For the study of energy consumption when a mobile robot travels on a curvature path, an initial and

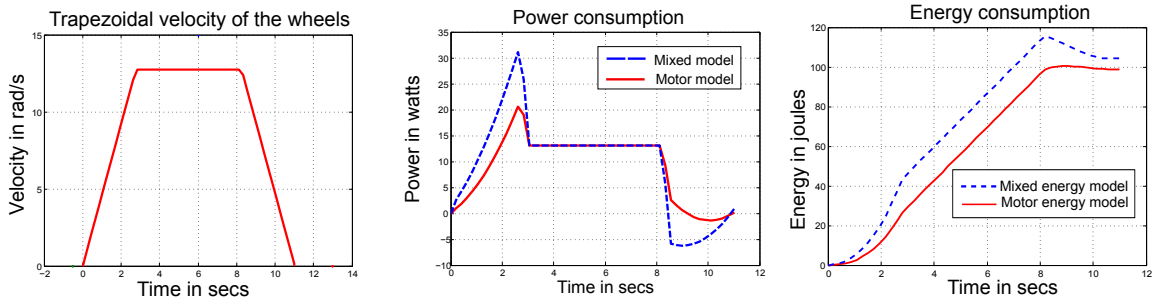

Figure 3: Simulation with a maximum trapezoidal angular velocity of the wheels (12.73 rad/s), maximum load weight carried by the mobile robot (7.6 kg), and a mobile weight of 6,04 kg, for a linear distance of 10 meters. (a) Trapezoidal angular velocity of the wheels (b) Power consumption given by the energy models. (c) Energy consumption given by the energy models.

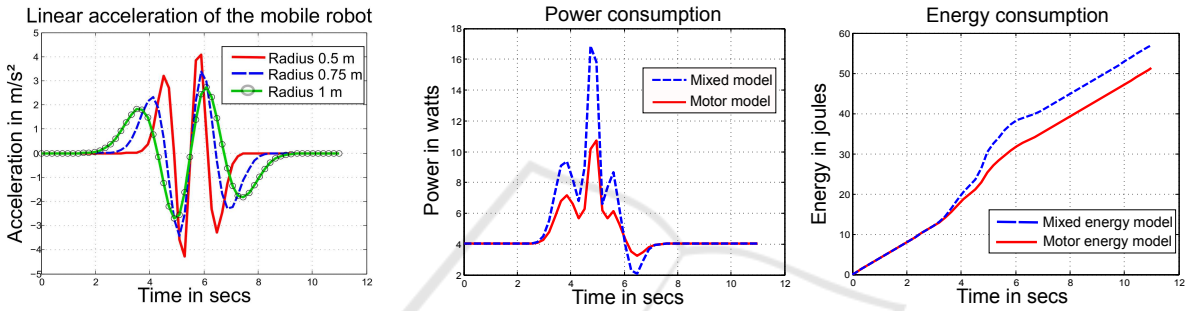

Figure 4: Simulation with a Gaussian function adapted to a circumference that delimited the obstacle, maximum load weight carried by the mobile robot (7.6 kg), and a mobile weight of 6,04 kg. (a) Linear acceleration of the wheels for the circumference radius of 0.5 m, 0.75 m, and 1 m. (b) Power consumption given by the energy models, for a radius circumference of 0.5 m. (c) Energy consumption given by the energy models, for a radius circumference of 0.5 m.

Table 4: Simulation results of the energy models with a different load weights.

Total weight	energy consumption	
Load and robot	Motor	Mixed
6.04 kg	71.9 J	73.15 J
9.8 kg	71.89 J	73.68 J
13.64 kg	71.88 J	74.25 J

Table 5: Energy consumption of the models when the radius circumference of the adapted Gaussian function changing.

Parameters		Energy consumption	
Radius	Distance	Motor	Mixed
0.5 m	7.06 m	51.26 J	56.96 J
0.75 m	7,17 m	50.13 J	52.04 J
1 m	7.28 m	50.74 J	51.66 J

goal position for the desired path is (x_d = 6, y_d = 4), the position of the circumference center is (x_c = 3, y_c = 2), the edge length of the obstacle cube is 0.7 meters. The only variable that changes for this study's proposes is the circumference radius that delimited the obstacle. In the Figure 4(a) is shows that the linear acceleration of the mobile robot is inversely related to the circumference radius, because a smaller radius represents a narrow bell of the adapted Gaussian function, forcing the mobile robot to accelerate to reach the peak. Is for that reason that in the table 5 with a smaller circumference radius, power and energy consumption is higher, despite the facts that, in the other cases, the travel distance is greater. Finally, in the Figure 4 the behavior of the energy models when travels on a curvature path remains the same as on the straight path, the mixed energy model increases its energy values compared to the motor energy model, when the mobile robot accelerate, because the dynamic parameters of the robot, are taken into consideration in the energy model proposed.

5 CONCLUSIONS

In this paper, an energy model that takes robot and motor dynamic parameters into account, is proposed. The energy consumption of the mixed energy model was compared to a typical motor energy model, using the angular velocities of the wheels as they relate related to the travel on straight and curvature paths. The simulation results show that the highest percentage of energy consumption came from the motors. However,

during mobile robot acceleration, the dynamic parameters of the robot, such as inertia moments, robot weight, or load weight, also influenced total energy consumption. It is for that reason that the energy values in figure 3 (b), (c), 4 (b), (c), and in tables 3, 4, 5 are higher in the mixed energy model than those of the DC motor energy model, because the proposed model consider the DC motor and the mobile robot dynamic models. However, in the deceleration phase, it was proven that a certain amount of energy was regenerated and stored in the batteries, allowing for the reduction of the total difference in energy consumption between energy models. A good estimation of power and energy consumption as presented, can be more easily related to the real-time autonomy of differential guide mobile robots, which carry their own energy source.

For the further study, the problem of testing the mixed energy model, on straight and curvature paths that minimize the energy consumption, and a experiment validation using the Nomad Super Scout mobile robot, remains.

REFERENCES

Dogru, S. and Marques, L. (2016). Power characterization of a skid-steered mobile field robot. In *International Conference on Autonomous Robot Systems and Competitions (ICARSC),4-6 May*, pages 15–20, Braganca, Portugal.

Dogru, S. and Marques, L. (2018). A physics-based power model for skid-steered wheeled mobile robots. In *IEEE Transactions on Robotics*, volume 34, pages 421 – 433.

Electro-Craft, C. (1977). *DC Motors, Speed Controls, Servo Systems: An Engineering Handbook.* Pergamon Press, USA, 3th edition.

G. Kladis, J. Economou, K. K. J. L. and Guerra, T. (2011). Energy conservation based fuzzy tracking for unmanned aerial vehicle missions under a priori known wind information. In *Engineering Applications of Artificial Intelligence*, volume 4, pages 278–294.

I. Bensekrane, P. Kumar, Y. A. and Merzouk, R. (2017). Towards adaptive power consumption estimation for over-actuated unmanned vehicles. In *IEEE International Conference on Robotics and Biomimetics*, pages 92–97, Macau SAR, China.

Kim, H. and Kim, B.-K. (2008). *Minimum-Energy motion planning for differential-driven wheeled Mobile Robots, Motion Planning*. Xing-Jian Jing (Ed.), ISBN: 978-953-7619-01-5, InTech, Croatia.

Liu, S. and Sun, D. (2014). Minimizing energy consumption of wheeled mobile robots via optimal motion planning, april. In *IEEE/ASME Transaction on Mechatronics*, volume 19, pages 401–411.

O. Chuy Jr., E.G Collins Jr., W. Y. and Ordonez, C. (2009). Power modeling of a skid steered wheeled robotic ground vehicle, 12-17 may. In *IEEE International Conference on Robotics and Automation*, pages 4118–4123, Kobe, Japan.

P. Tokekar, N. K. and Isler, V. (2014). Energy-optimal trajectory planning for car-like robots. In *Autonomus Robots Journal*, volume 37, pages 279–300.

Yamamoto, Y. and Yun, X. (1994). Coordinating locomotion and manipulation of a mobile manipulator. In *IEEE Transactions on Automatic Control*, volume 39, pages 1326–1332.

Yun, X. and Yamamoto, Y. (1993). Internal dynamic of a whelled mobile robot. In *IEEE/RSJ International Conference on Intelligent Robots and Systems*, pages 1288–1294, Yokohama, Japan.